Evaluation of Two Gustiness Models for Exposure Correction Calculations

J. W. Verkaik
Royal Netherlands Meteorological Institute (KNMI)
PO Box 201, 3730 AE De Bilt, Netherlands.
Phone: +31 30 2206 864. Fax: +31 30 2204 614.
E-mail: job.verkaik@knmi.nl

October 7, 1999

published in
Journal of Applied Meteorology
Volume 39, No. 9, pages 1613-1626, 2000.

Abstract

Gustiness models from Wieringa and Beljaars are evaluated. The models are used to relate the gustiness from wind speed records to the local roughness length. The roughness length is used to apply exposure corrections to sheltered wind stations. The gustiness models are mutually compared and the influence of measuring chain inertia and the measuring period on the measured gusts is evaluated. Beljaars's model is used to estimate the wind speed at elevated levels from wind speed and gustiness records measured close to the surface. Uncertainties in the computation of roughness lengths from gustiness records are also evaluated. For measuring periods of 1 h the exposure corrections from the two models are equal over smooth terrain. Over rough terrain Beljaars's gustiness model yields smaller corrections, differences up to 10% are possible. For 10-min periods Beljaars's corrections are 3%–10% smaller than those of Wieringa. Other uncertainties, resulting from the assumption of neutral stratification and a value for the blending height, are smaller than 5%.

1. Introduction

When wind speed observations measured at different locations are compared, corrections for differences in site exposure are necessary. For this purpose, information on the local roughness or the distribution of obstacles and roughness patches in the station's environment is a prerequisite. Different methods for site exposure corrections are available. Wieringa (1986, 1996) used observed gustiness data for exposure correction computation. When detailed information on the station's environment is available, it can be used to estimate the local wind speed profile. This was done, for example, by Wolfson and Fujita (1989), using obstruction angles as measured from panoramic photographs. Troen and Petersen (1989) developed a method with inclusion of an internal boundary layer model, which make the method applicable in regions downwind of major roughness changes,for example, the coastal zone. Miller et al. (1998) use a combination of an internal boundary layer model, a model for topographic effects and an altitude factor to correct the United Kingdom anemographs for site exposure. A problem is that the station's environment may change in time. Growing trees or approaching builtup areas may cause a gradual increase in surface roughness. For climatological records of wind speed these changes are usually poorly documented.

An abundance of information on the local boundary layer structure can be extracted from raw turbulence data, even when measured at a single height (Sozzi et al. 1998). For operational meteorological stations this kind of data will generally not be available. Roughness lengths can also be derived from profile measurements of average wind speed when these are available for the site of interest. This will usually not be the case for regular meteorological stations, however.

The roughness at a meteorological site can be deduced from the turbulent wind speed fluctuations. In the neutral, homogeneous surface layer the horizontal wind speed U is a

logarithmic function of height z (Tennekes 1973)

$$U = \frac{u_*}{\kappa} \ln \frac{z}{z_0}, \tag{1}$$

where the von Kármán constant $\kappa = 0.4$ (Frenzen and Vogel 1995), and u_* is the friction velocity, related to the momentum flux, $u_*^2 = -\overline{u'w'}$ (u' and w' are turbulent fluctuations of the horizontal and vertical wind speed, respectively). In surface layers over homogeneous terrain z_0 is well defined and u_* is constant with height. The standard deviation of horizontal wind speed σ_u scales with u_* and is a function of stability (L, Monin–Obukhov length) and the boundary layer height (z_i)

$$\sigma_u/u_* = c\,(z/L, z_i/L)\,, \tag{2}$$

with $c \simeq 2.2$ in the neutral limit ($|L| \to \infty$). When σ_u and U are measured simultaneously, combination of Eqs. (1) and (2) yields the roughness length. Horizontal wind speed fluctuations in the surface layer are partially generated locally through mechanical turbulence, and are partially the result of eddies with the size of the boundary layer height. Since large eddies adjust only slowly to new surface properties, σ_u is influenced by an upwind fetch with the magnitude of the boundary layer height (Højstrup 1981, Beljaars 1987b).

Climatological records of wind speed usually do not include σ_u observations. Only recently do automatic weather stations (AWS) record σ_u, and this will simplify the computation of exposure corrections considerably in the future. Earlier datasets provide gustiness measurements only. This is the only parameter that has been recorded routinely at meteorological stations that carries turbulence information.

Wieringa's gustiness model, presented in Wieringa (1973, 1976, 1977), was explicitly derived for the purpose of exposure corrections and applied in the wind climate assessment of the Netherlands (Wieringa and Rijkoort 1983). However, this model cannot be used when the wind speed is discretely sampled, as is the case at the stations of the Royal Netherlands Meteorological Institute (KNMI) since the early 90s. Beljaars's model, presented in Beljaars (1987a, 1988), seems a good alternative for Wieringa's model, but Beljaars did not use his model for site exposure corrections. The purpose of the present paper is to compare the two models and assess the possible difference in resulting roughness and exposure correction estimates. Gustiness data from three inland stations in the Netherlands are analyzed. Exposure corrections are necessary when the station's environment is inhomogeneous. Strictly speaking the application of Monin–Obukhov similarity theory (M–O theory) is not appropriate over inhomogeneous terrain, but for want of something better it will be used throughout this paper. Wieringa assumes a Gaussian distribution for the instantaneous wind speed [$U(t)$] and Beljaars assumes that $U(t)$ and its time derivative ($\partial U/\partial t$) are joint Gaussian. Turbulence in the atmospheric boundary layer is not fully Gaussian as $\partial U/\partial t$ is not normally distributed (Panofsky and Dutton 1984). Kristensen et al. (1991) argue, however, that $U(t)$ and $\partial U/\partial t$ are uncorrelated and that their joint probability may still be Gaussian.

The present study is a contribution of KNMI to the HYDRA-project (RIKZ[1]–RIZA[2]). In the HYDRA-project the hydraulic boundary conditions are assessed for safety testing of the Dutch dams. Updating of the Dutch wind climate assessment by Wieringa and Rijkoort (1983) is one of the main goals of the KNMI contribution.

2. Exposure correction

Exposure corrections can be made when the local roughness length is known (Wieringa 1976, 1977, 1986, 1996, Oemraw 1984), as will be explained next. The measured wind speed U_{m} at height z_{m} is extrapolated from the surface to a level z_{b} using the logarithmic velocity profile (Eq. 1). The wind speed at z_{b} (U_{b}) is assumed to be horizontally constant, and the level z_{b} is therefore called the "blending height": the effects of all surface inhomogeneities have blended into the mean flow. The wind speed at the blending height can be estimated from

$$U_{\mathrm{b}} = U_{\mathrm{m}} \frac{\ln z_{\mathrm{b}}/z_0}{\ln z_{\mathrm{m}}/z_0}. \tag{3}$$

This wind speed can now be used to calculate the "potential wind speed": the wind speed at $z_{\mathrm{ref}} = 10$ m height over open terrain (grass, $z_{0\mathrm{ref}} = 0.03$ m):

$$U_{\mathrm{p}} = U_{\mathrm{b}} \frac{\ln z_{\mathrm{ref}}/z_{0\mathrm{ref}}}{\ln z_{\mathrm{b}}/z_{0\mathrm{ref}}}. \tag{4}$$

The potential wind speed is a reference wind speed, free of local effects. The exposure correction factor S is given by the ratio of $U_{\mathrm{p}}/U_{\mathrm{m}}$:

$$S = \frac{U_{\mathrm{p}}}{U_{\mathrm{m}}} = \frac{\ln z_{\mathrm{b}}/z_0}{\ln z_{\mathrm{m}}/z_0} \frac{\ln z_{\mathrm{ref}}/z_{0\mathrm{ref}}}{\ln z_{\mathrm{b}}/z_{0\mathrm{ref}}}. \tag{5}$$

In Fig. 1 the wind speed profiles are plotted for the case $z_0 = 0.5$ m, $z_{\mathrm{m}} = z_{\mathrm{ref}} = 10$ m, and $z_{\mathrm{b}} = 60$ m. The uncertainties that are inherent to this method concerning z_{b} and the influence of stability on U and c are assessed in section 7. As was already stated, M–O theory is used even though this may not be quite exact over heterogeneous surfaces.

In the process of exposure correction computation, gustiness analysis is an additional step to come to the ratio σ_u/U. When direct observation of σ_u become available one might expect an increased accuracy in z_0 estimation. However, Barthelmie et al. (1993) estimated the wind speed at higher level on a mast from the wind speed at 12 m. They compared profile, gustiness, standard deviation methods, and z_0 evaluation from land use maps and found that direct measurements of σ_u/U yielded the worst results of all methods.

[1]Rijksinstituut voor Kust en Zee = National Institute for Coastal and Marine Management

[2]Rijksinstituut voor Integraal Zoetwaterbeheer en Afvalwaterbehandeling = Institute for Inland Water Management and Waste Water Treatment

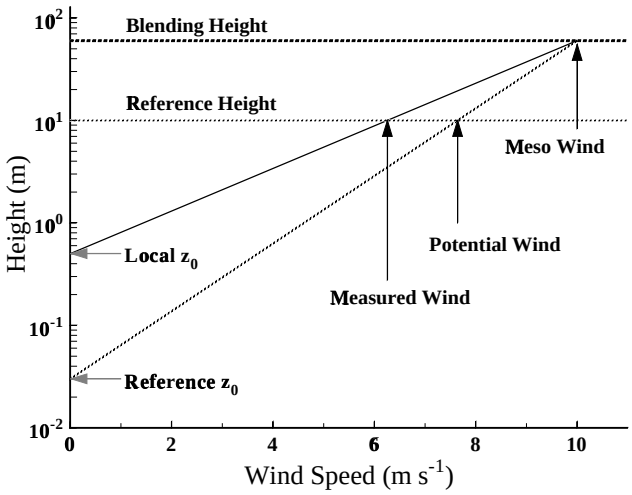

Figure 1: Wind speed profile with local $z_0 = 0.5$ m and $z_\mathrm{m} = z_\mathrm{ref} = 10$ m.

3. Gustiness models

The gustiness parameter G is defined as follows

$$G \equiv \frac{U_\mathrm{max}}{\overline{U}}, \tag{6}$$

where $\overline{U}$ is the average wind speed during the period that the gust U_max appeared. The normalized gust

$$u_x = \frac{U_\mathrm{max} - \overline{U}}{\sigma_u}, \tag{7}$$

is solely determined by the variance spectrum of atmospheric turbulence (which is a function of stability), and the anemometer–transmission–recorder system which comprises the "measuring chain." The measuring chain can be considered as a filter with certain time- and/or length scales, associated with the response length of the anemometer and the response time of the recorder. When neutral stability is assumed and the time- and length scales of the measuring chain are known, the average $\overline{u_x}$ or median $\langle u_x \rangle$ of u_x can be computed. From the logarithmic wind speed profile [Eq. (1)] and the relation between u_* and σ_u [Eq. (2)], we can express G as function of z_0

$$\frac{\sigma_u}{\overline{U}} = \frac{c\kappa}{\ln z/z_0}, \qquad \text{so} \tag{8}$$

$$G = 1 + \frac{U_\mathrm{max} - \overline{U}}{\overline{U}} = 1 + \frac{\sigma_u}{\overline{U}} \frac{U_\mathrm{max} - \overline{U}}{\sigma_u} = 1 + \frac{c\kappa}{\ln z/z_0} u_x. \tag{9}$$

Note that if we use $c = 2.5$, $c\kappa = 1$. The filtering of the wind speed signal by the measuring chain will modify the shape of the spectrum, attenuating more strongly the higher frequencies.

This effect reduces G and $\langle u_x \rangle$. The inertia of the measuring chain also changes the apparent value of $\sigma_u/\overline{U}$ by a factor A. This attenuation can be expressed as $\sigma_{u\mathrm{m}}/\sigma_u$, where $\sigma^2_{u\mathrm{m}}$ is the variance that will be transmitted by the measuring chain. As in the gustiness models that will be considered this factor A is accounted for in different ways, it is not included in Eq. (9).

Wieringa (1973) and Beljaars (1987a) derived expressions for u_x. Wieringa's model has less statistics, only a random-data exceedance criterion with expanded physical modeling, while Beljaars's derivation is more statistically based. Both incorporate the effect of filtering on the measured gustiness, since only gustiness parameters together with a duration or length specification (spatial or temporal filtering) are useful. Wieringa considers only the process of analog recording, Beljaars discusses also discrete sampling. Next both methods will be outlined.

4. Wieringa's gustiness analysis

a. The gustiness model

The median gust ($\langle u_x \rangle$) recorded by an anemometer–recorder combination in a certain time period (T) has a probability of exceedance of $1/2N$, where N is the number of independent gust observations in period T. In other words, when again N gust observations are taken, 50% will have a larger u_x. For a normal distribution, $\langle u_x \rangle$ can be expressed as a function of N. Wieringa (1973) summarizes integral calculations by Parratt (1961):

$$\langle u_x \rangle = 1.42 + 0.301 \ln (N - 4), \qquad \text{for } N > 7. \tag{10}$$

The number of independent gust observations N in period T will be a function of T and the duration of the gust. As atmospheric turbulence is described with length scales rather than timescale we can also state

$$N \sim \frac{\text{length scale}}{\text{gust length}}. \tag{11}$$

Wieringa expressed the gust length as $\overline{U} t_{\mathrm{gust}}$. Here t_{gust} is the gust duration. Note that the gust length $\overline{U} t_{\mathrm{gust}}$ is different from $U_{\max} t_{\mathrm{gust}}$.

From detrended 1-Hz turbulence measurements over wide open water during strong winds, Wieringa determined values of z_0 and G resulting in $N = 87$ and a length scale of 990 m for averaging periods of 10 min. He assumed that for extension of T the turbulence-related parameters z and z_0 are less relevant, and climatological statistics are adequate for finding the gust factor increase with increasing averaging period. Taking $\langle u_x \rangle = 1.73$ for $N = 6$, and using 10-min sampled experimental wind data with $(\sigma_u/U) \approx 0.06$ related to 1-h averaging periods, Wieringa scaled the total expression for $G_{\text{10-min}}$ with a factor f_T, which is unity for $T = 10$ min and 1.10 for $T = 1$ h. Wieringa's final gust model, fitting well to all reliable

published G data then available, is

$$\langle G \rangle = f_T \left[1 + \frac{1.42 + 0.301 \ln \left(990 \text{ m} / \overline{U} t_{\text{gust}} - 4 \right)}{\ln z / z_0} \right]. \tag{12}$$

Wieringa (1973) was based on high-speed research data, and to account for the slower response of operational anemometry an attenuation factor A was introduced in later papers (Wieringa 1976, 1977, 1986). Wieringa also adjusted the length scale from 990 to 1000 m. For anemometer response length λ and analog recorder response time t_{rec} the attenuation factor is

$$A = \left[1 + \left(2\pi\lambda / U t_{\text{gust}} \right)^2 \right]^{-1/2} \left[1 + \left(2\pi t_{\text{rec}} / t_{\text{gust}} \right)^2 \right]^{-1/2}. \tag{13}$$

The attenuation should only be applied to fluctuations of wind , so

$$G_{\text{meas.}} - 1 = A \left(G_{\text{wind}} - 1 \right). \tag{14}$$

In context of Wieringa's model the factor A is not the fraction transmitted variance of σ_u, but the transmission of the measuring chain for gusts with duration t_{gust} or length $\overline{U} t_{\text{gust}}$.

In period T, gusts of all magnitudes will be present. When gustiness observations are used to calculate z_0, it is necessary to know the gust length to be used in Eq. (12). The damping of gusts due to anemometer and recorder inertia is a function of gust duration: short gusts (large G) will be attenuated more strongly than long gusts (small G). As a result G will not increase when $\overline{U} t_{\text{gust}}$ goes to zero, but, according to Wieringa (1976), there will be a maximum in the recorded G below which the attenuation by anemometer and recorder becomes dominant. The $\overline{U} t_{\text{gust}}$ to be used in Eq. (12) is the gust length at which the maximum occurs of the product of u_x and A:

$$u_x A = \left[1.42 + 0.301 \ln \left(\frac{990 \text{ m}}{\overline{U} t_{\text{gust}}} \right) \right] \times \left[1 + \left(2\pi\lambda / U t_{\text{gust}} \right)^2 \right]^{-1/2} \left[1 + \left(2\pi t_{\text{rec}} / t_{\text{gust}} \right)^2 \right]^{-1/2}. \tag{15}$$

By putting the derivative of this expression to t_{gust} at zero, an expression for the gust length can be found. Oemraw (1984) gives calculator programs for deriving $t_{\text{gust}}(U)$ from λ and t_{rec}, Wieringa (1976, 1980) gives nomograms for finding t_{gust} from such calculations. Typically in Wieringa's model the gust duration will be one or two orders of magnitude larger than the response time of the recorder, depending on U.

b. Comments on Wieringa's model

The following must be noted concerning Wieringa's gust model. When the probability density distribution of wind speed is Gaussian,

$$P(U) = \frac{1}{\sigma_u \sqrt{2\pi}} \exp \left[- \left(\frac{U - \overline{U}}{\sigma_u \sqrt{2}} \right)^2 \right], \tag{16}$$

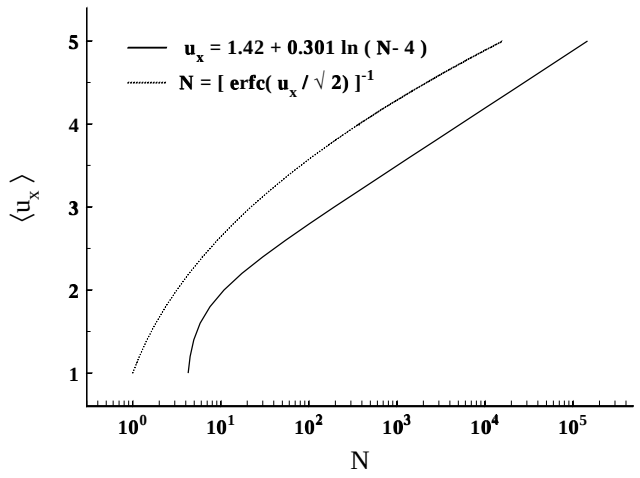

Figure 2: The u_x with chance of exceedance $1/2N$ as function of N.

the chance of exceeding $U_{\max}$ equals (Abramowitz and Stegun 1965)

$$P(U > U_{\max}) = \frac{1}{2}\left[\frac{2}{\sqrt{\pi}}\int_{\frac{u_x}{\sqrt{2}}}^{\infty} e^{-t^2}dt\right] = \frac{1}{2}\left(\text{erfc}\ \frac{\langle u_x\rangle}{\sqrt{2}}\right), \tag{17}$$

where erfc is the complementary error function. We are looking for the number of samples N so that $P(U > \langle U\rangle) = 1/2N$. So

$$N\left(\langle U\rangle\right) = \left[2P(U > \langle U\rangle)\right]^{-1} = \left[\text{erfc}\ \frac{\langle u_x\rangle}{\sqrt{2}}\right]^{-1}. \tag{18}$$

This expression must be compared with Wieringa's (1973) expression [Eq. (10)]. In Fig. 2 both functions are plotted. For a given N Eq. (10) yields lower estimates of $\langle u_x\rangle$ than Eq. (18) (B. Wichers Schreur, KNMI, pers. comm.). Proceeding in Wieringa's derivation of Eq. (12) this difference becomes unimportant, however, because Wieringa "tunes" the factor $990/\overline{U}t_{\text{gust}}$ to yield the correct z_0 for his dataset.

To derive a gust length Wieringa applies the attenuation function A to his gust model. This is done using a single time or length scale. Wieringa describes the gust length as the length scale at which the measured gusts are strongest. In fact, A is a spectral transfer function and gusts are the result of the superposition of fluctuations with a variety of length scales. Moreover, gusts occur in the time domain whereas A is defined in the spectral domain. As we will see later, the gust length is a cutoff scale. Gusts smaller than this scale will have less influence on G because of the attenuation by the measuring chain.

5. Beljaars's gustiness analysis

a. The gustiness model

Beljaars's (1987a) starting point is the assumption that $U(t)$ and $\partial U/\partial t$ are joint Gaussian. In that case the probability of u_x being less than some arbitrary level U_s in period T is

$$P\left(u_x < U_s, T\right) = \exp\left[-E\left(U_s, T\right)\right], \tag{19}$$

$$E\left(U_s, T\right) = \nu T e^{-U_s^2/2}. \tag{20}$$

Here E is the expected number of upcrossings of level U_s, ν is a frequency, the zero-crossing rate of $U - \overline{U}$, corresponding to the width of the power spectrum of horizontal wind speed variance,

$$\nu^2 = \frac{\int_0^\infty n^2 S_u(n) dn}{\int_0^\infty S_u(n) dn}. \tag{21}$$

Here S_u is the spectral density at frequency n. For large νT the *average* $\overline{u_x}$ equals

$$\overline{u_x} = \left(2 \ln \nu T\right)^{1/2} + \gamma \left(2 \ln \nu T\right)^{-1/2}, \tag{22}$$

where $\gamma = 0.5772$ (Euler's constant). The first term on the right-hand side of Eq. (22) is the mode of u_x.

Spectra, necessary for the evaluation of ν, can be taken from literature. Beljaars used spectra from Kaimal (1977, data from the Minnesota site). These spectra explicitly include the influence of the boundary layer height z_i on the low-frequency part of the spectrum. The high-frequency portion scales on surface-layer parameters only, and there is a transition zone:

$$\frac{nS_u(n)}{u_*^2} = \begin{cases} \left(1 + 0.75 \left|\dfrac{z}{L}\right|^{2/3}\right) 0.3 f^{-2/3} & f \geq \dfrac{1}{2}, \\ \left(1 + 0.75 \left|\dfrac{z}{L}\right|^{2/3}\right) 0.48 \left(2f\right)^{-p} & \dfrac{1}{2} \geq f \geq \dfrac{3z}{2z_i}, \\ \left(12 + 0.5 \left|\dfrac{z_i}{L}\right|\right)^{2/3} \dfrac{f_i}{1 + 3.1 f_i^{5/3}} & f \leq \dfrac{3z}{2z_i}. \end{cases} \tag{23}$$

Here the dimensionless frequencies f and f_i are given by $nz/\overline{U}$ and $nz_i/\overline{U}$, respectively. Here L is the Monin–Obukhov length:

$$L = -\frac{u_*^3 \theta}{\kappa g \overline{w'\theta'}}, \tag{24}$$

where g is the acceleration of gravity (9.8 m s^{-2}), θ is the potential temperature, and $\overline{w'\theta'}$ is the kinematic heat flux. For the transition zone p is given by

$$p = \ln\left(0.44 \frac{\left(12 + 0.5\left|z_i/L\right|\right)^{2/3}}{1 + 0.75\left|z/L\right|^{2/3}}\right) \Big/ \ln\left(\frac{z_i}{3z}\right). \tag{25}$$

The transfer function of the anemometer ($\tau = \lambda/\overline{U}$) or recorder ($\tau = t_{\rm rec}$) for ${\sigma_u}^2$ as function of frequency is a regular first order transfer function, and can be written as

$$T_1(n) = \left[1 + (2\pi n\tau)^2\right]^{-1}. \tag{26}$$

The transfer function of an analog running-average filter over t_0 s is

$$T_{\rm ra}(n) = \left(\frac{\sin \pi n t_0}{\pi n t_0}\right)^2, \tag{27}$$

and for a discrete running-average

$$= \left(\frac{\sin \pi n \Delta N}{N \sin \pi n \Delta}\right)^2. \tag{28}$$

Here averaging is done over N samples taken at Δ s intervals (ΔN is the averaging period).

When the wind speed signal is discretely sampled, the maximum will generally be missed, so $\overline{u_x}$ will be smaller than with continuous recording. Beljaars derived a modified expression for Eq. (20) by considering the expected number of upcrossings of a linearly interpolated signal between successive samples:

$$E\left(U_s, T\right) = \frac{T}{\Delta} \mathrm{P}\left(u_x\left(t\right) < U_s, u_x\left(\ t + \Delta\right) > U_s\right), \tag{29}$$

from which he derived

$$E\left(U_s, T\right) = \frac{T}{\Delta}\frac{1}{\pi}\int_0^a \frac{\exp\left[-\frac{1}{2}U_s^2\left(1+y^2\right)\right]}{1+y^2} dy, \tag{30}$$

where

$$a = \left(\frac{1-\rho}{1+\rho}\right)^{\frac{1}{2}}, \text{ and } \quad \rho = \frac{R\left(\Delta\right)}{R\left(0\right)}. \tag{31}$$

Here R is the autocovariance of the wind speed signal and can be computed from the turbulence spectrum. A new expression for $\overline{u_x}$ can now be derived:

$$\overline{u_x} = \left(2\ln\frac{Ta}{\Delta\pi}\right)^{1/2}\left(1 - \frac{1}{6}a^2\right) + \gamma\left(2\ln\frac{Ta}{\Delta\pi}\right)^{-1/2}. \tag{32}$$

For small Δ

$$\lim_{\Delta\to 0}\frac{a}{\Delta\pi} = \nu, \qquad \lim_{\Delta\to 0} a = 0, \tag{33}$$

and Eq. (32) reduces to Eq. (22).

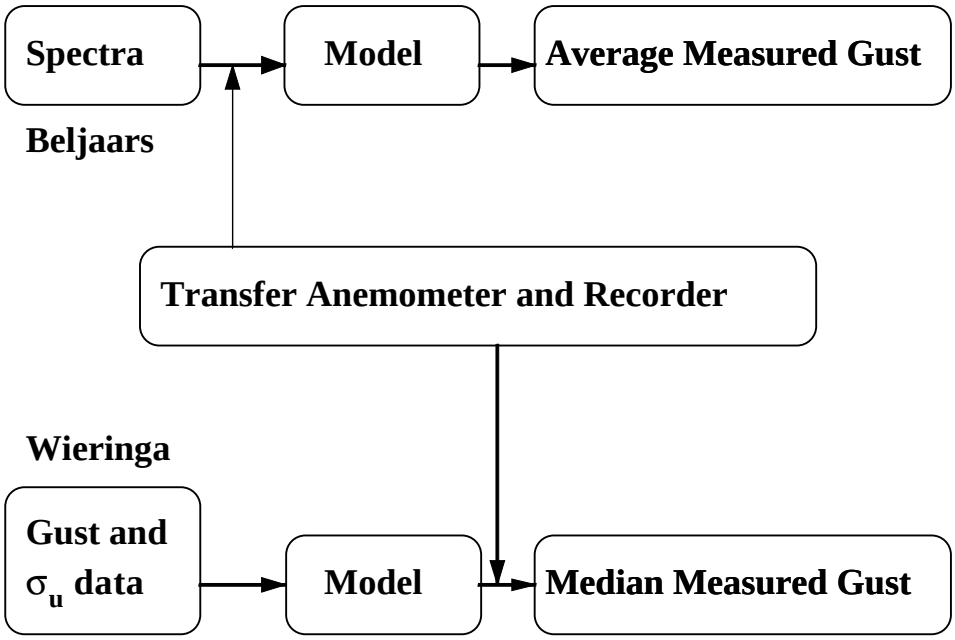

Figure 3: Flow chart showing the different concepts of Wieringa and Beljaars.

b. Comments on Beljaars's model

There are two major differences between Wieringa's and Beljaars's model: the first concerns the influence of the measuring period T, and the second concerns the attenuation factor A.

The influence of T on u_x enters Beljaars's model via Eqs. (22) and (32). It also influences the apparent value of c, σ_u is high-pass filtered with time constant T as an additional attenuation to A. In Wieringa's model the influence of T on the measured gustiness enters the equations by the factor f_T in Eq. (12). As we will see in the next section this difference hampers the direct comparison of the u_x values from both models.

To stress the conceptual difference between Beljaars's and Wieringa's model concerning the transfer function A, in Fig. 3 a flow chart is plotted. Wieringa's method starts with a statistical criterion and uses gustiness data to find $u_x(\overline{U}t_{\mathrm{gust}})$, then he applies the recorder and anemometer transfer functions to find $\overline{U}t_{\mathrm{gust}}$ and hence the expected $\langle u_x \rangle$.

Beljaars's method starts with spectra. All transfer functions have to be applied to the turbulence spectrum. These modified spectra enter the gust model, which yields the expected average $\overline{u_x}$ (Greenway 1979, cf. Fig. 2). The anemometer and recorder transfer will influence ν via Eq. (21), and $\overline{u_x}$ via Eq. (22). This also applies to the running-average filter.

The effect of the anemometer inertia on u_x according to Beljaars's model is illustrated

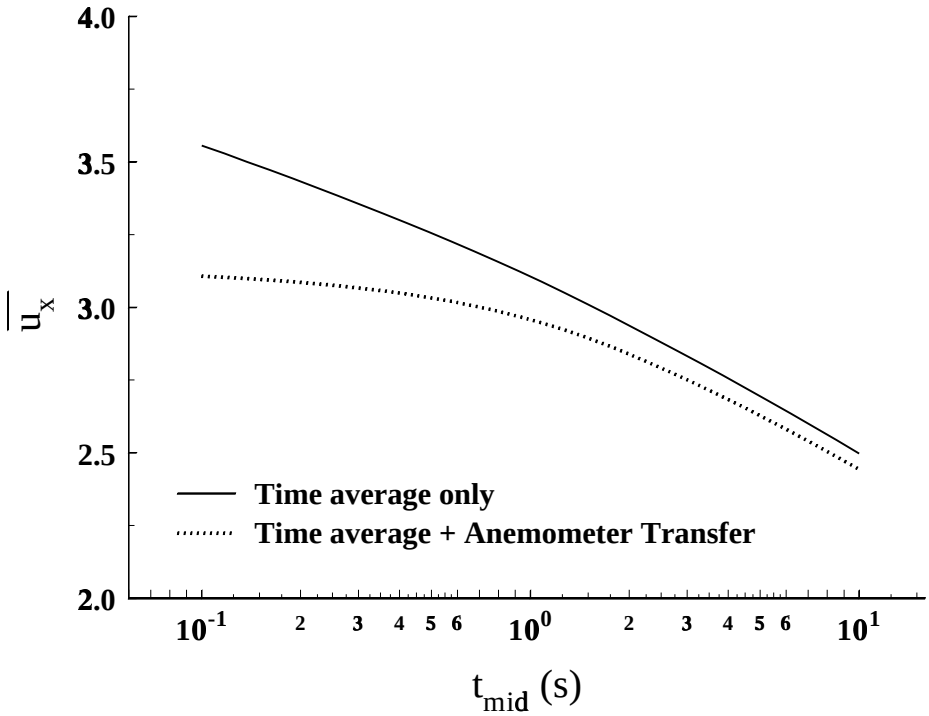

Figure 4: Averaged normalized gust magnitude $\overline{u_x}$ as function of averaging time of running-average filter with and without application of the anemometer transfer function.

in Fig. 4. Here $\overline{u_x}$ is plotted as function of the averaging time of the running-average filter with and without application of the anemometer transfer function ($U = 8$ m s^{-1}, $\lambda = 4$ m). Both the running-average over time and the anemometer will attenuate high frequencies in the turbulence signal, and this will reduce the expected $\overline{u_x}$. Shorter averaging times will yield a larger $\overline{u_x}$, also when this averaging time is smaller than the anemometer response time (4 m/8 m s^{-1} = 0.5 s). This figure shows that fluctuations of all scales, even the smallest, will contribute to $\overline{u_x}$. So the peak gust in a record cannot be associated with a single gust length. However, the main contribution to the variance in the recorded signal will come from fluctuations with length scales comparable with the length scale of the measuring chain. So the gust duration of a measuring chain is the cutoff time below which the gusts are strongly attenuated. Beljaars (1987a, 1988) defines the gust duration as follows:

> Gusts observed after a running-average filter have a duration that is equal to the averaging time of the filter. An arbitrary measuring chain with several elements (not necessarily running-average filters) produces gusts with duration t_0, if a hypothetical running-average filter with averaging time t_0 would have resulted in the same gust magnitude.

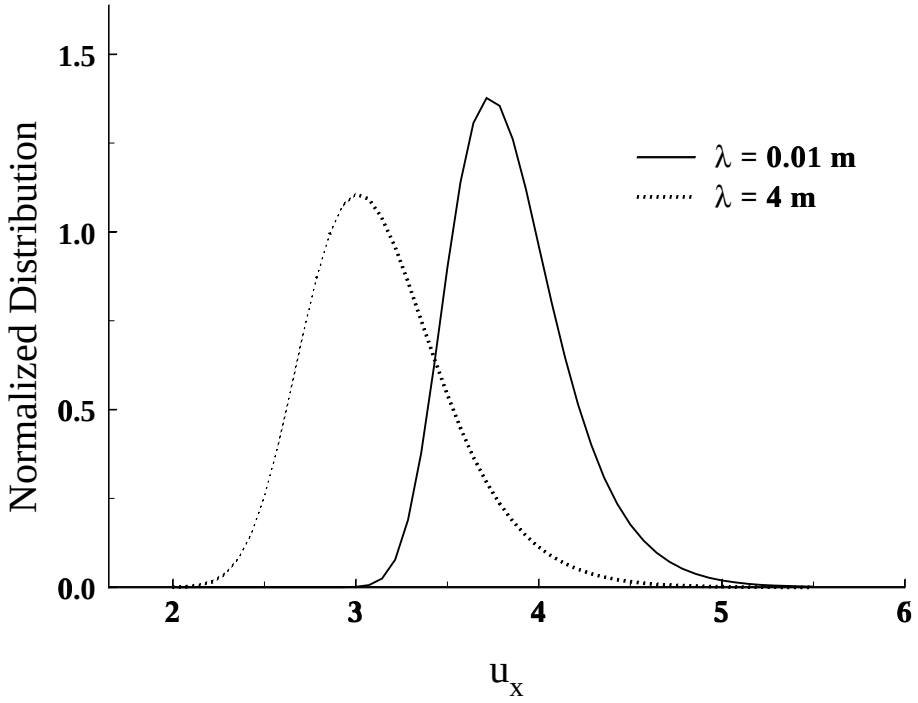

Figure 5: Normalized distribution of u_x for two measuring chains, the first with an anemometer response length of 0.01 m, the second with a response length of 4 m. For both a recorder response time of 0.001 s was used.

The effect of anemometer inertia on the observed gusts distribution is illustrated in Fig. 5. Here the normalized distribution of u_x is plotted [Eq. (19)] for two measuring chains. Filtered gusts have smaller u_x. The shift in the average of u_x corresponds to the difference between the curves in Fig. 4.

6. Application of gustiness models

In this section the gustiness models will be used for roughness length estimation, this z_0 is used to compute the exposure correction. Beljaars's model was not designed for z_0 estimation. The application is straightforward and similar to that of Wieringa's model, however. Maximum gust records and information on the measuring chain is the required input information, just as in Wieringa's model.

In the context of Beljaars's model, the factor A reduces the apparent value of $\sigma_u/\overline{U}$, the

second term in Eq. (9). Then from rearranging Eq. (9) we can derive

$$\ln \frac{z}{z_0} = \frac{Ac\kappa u_x}{G-1}, \tag{34}$$

which yields the roughness length. The attenuation A can be computed from

$$A^2 = \frac{\int_0^\infty T_{hp}(n) T_1(n) T_{\mathrm{ra}}(n) S_u(n) dn}{\int_0^\infty S_u(n) dn}, \tag{35}$$

where T_{hp} is the high-pass filter associated with the measuring period T:

$$T_{hp}(n) = 1 - \left[1 + (2\pi n T)^2\right]^{-1}. \tag{36}$$

In the context of Wieringa's model, combination of Eqs. (12) and (14) leads to

$$\ln \frac{z}{z_0} = \frac{f_T Ac\kappa u_x}{G - 1 - A(f_T - 1)}. \tag{37}$$

Now A is given by Eq. (13). The additional term in the denominator is the result of the time function f_T operating on the total right-hand side of Eq. (12), in stead of working on the turbulent fluctuations alone like the attenuation A does. The peculiar result is an interaction between A and f_T: the value of f_T determines to what extent A influences the measured gustiness. In case of $T = 3600$ s, $f_T = 1.1$. With $A \approx 0.9$ and $G - 1 \approx 0.5$, it is clear that the term $A\,(f_T - 1)$ has a major influence on the roughness length estimate.

For both models knowledge of the average wind speed is necessary. So when G is determined, a selection on a certain wind speed range should be applied. The wind speeds selected should not be too low, to ensure nearly neutral conditions. For the Netherlands, with only weak or moderate insolation, a minimum wind speed of 5 m s^{-1} is usually enough. De Bruin et al. (1993) computed z_0 from measurements of σ_u and U using Eq. (8) for a site in southern France. Their Fig. 10 shows that even in cases of strong insolation a wind speed of 7 m s^{-1} is enough to let z_0 converge to a single value. Note that for Wieringa's model the median, and for Beljaars's model the average, of G and u_x should be taken. The difference is usually insignificant for the exposure correction estimates, however. An advantage of using the median is it's stability in nonstationary situations.

The evaluation of the models is done in four ways. First, for three measuring chains the relation between G, z_0, and S is investigated. The measuring chains are examples from routine observations that have been used at different KNMI stations in the past. Second, the effect of the measuring period T is investigated by analyzing a dataset from Schiphol (Amsterdam airport). Third, a record from Zestienhoven (Rotterdam airport) is used to evaluate the models's capacity to deal with changes in the measuring chain. Fourth, the roughness lengths found with Beljaars's model are used to estimate the wind speed at 40- and 80-m height, the region of the assumed blending height, from the wind speed at 10-m height at the Cabauw tower (Van Ulden and Wieringa 1996). The estimates are then compared with the observed wind speed at these height.

Chain	λ (m)	Recording	Recorder parameters
1.	2.9	Continuous	$t_{\rm rec} = 0.8$ s
2.	2.9	Continuous	$t_{\rm rec} = 0.2$ s
3.	2.9	Discrete	$\Delta = 0.25$ s, $N = 12$

Table 1: Input parameters for three measuring chains.

$z_{\rm m}$	$z_{\rm b}$	$z_{\rm i}$	L	T	U
10 m	60 m	1000 m	-10^5 m	3600 s	8.2 m s^{-1}

Table 2: Input parameters for spectra and exposure correction computation.

a. Evaluation of three measuring chains

In this section the two gustiness models are evaluated for three measuring chains. In all cases a cup anemometer (KNMI 018, $\lambda = 2.9$ m) is used, first in combination with a Nieaf recorder, second with a Camille Bauer recorder, and third with the AWS configuration. The parameters of these measuring chains can be found in Table 1. Since the latter measuring chain samples at discrete time intervals, it will only be evaluated with Beljaars's model. In Table 2 the necessary parameters of the atmospheric boundary layer are given. When calculating z_0 with Beljaars's model we use $c = \sigma_u/u_* = 2.2$, and with Wieringa's model $c = 2.5$, since these are the values used by the authors themselves.

Wieringa's roughness lengths are larger than those resulting from Beljaars's model (see Fig. 6). The resulting exposure correction factors are plotted in Fig. 7a. Over smooth terrain, when the exposure correction is less than 1, Wieringa's correction is about 1% larger than (chain 1), or is equal to Beljaars's correction (chain 2). Over rough terrain Wieringa's correction is larger by about 12% (chain 1) or 7% (chain 2).

To illustrate the effect of the term $A\,(f_T - 1)$ in the denominator of Eq. (37), Fig. 7a is recomputed and plotted in Fig. 7b for the same measuring chains with the only difference that $T = 600$ s instead of $T = 3600$ s. So $f_T = 1$ and the $A\,(f_T - 1)$ in the denominator of Eq. (37) vanishes. A different gustiness interval has been chosen so that the same range of exposure corrections factors (and roughness lengths) is obtained. Again Wieringa's exposure correction is larger, 3% or 2% for smooth surfaces to 12% or 9% for rough surfaces for chain 1 and 2, respectively.

So with $z_0 = 0.1$ m Wieringa's correction is about 6% larger. However, since $\langle G \rangle$ is a few percent smaller than $\overline{G}$, this difference is reduced to 4%–5%.

b. Schiphol dataset

In the previous section it was shown that the difference between Beljaars's and Wieringa's exposure corrections is a function of the measuring time T. In this section the influence of T

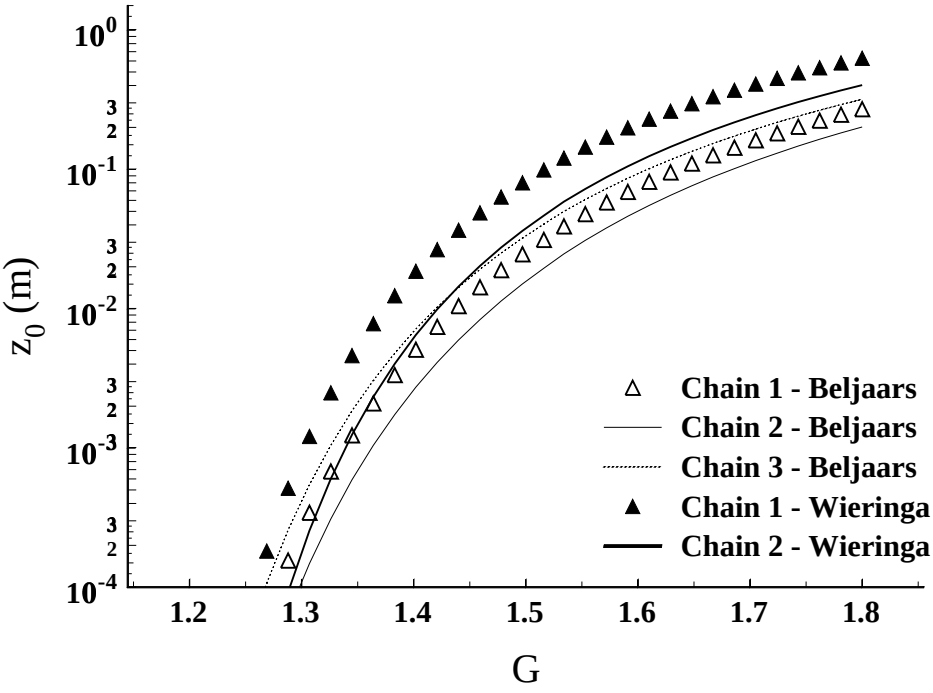

Figure 6: Roughness length as function of G calculated using Beljaars's and Wieringa's model for the three measuring chains of section 6a with $T = 3600$ s.

will be investigated further. This will be done using a dataset collected at Schiphol airport. The data were collected on four masts of 10-m height by analog recorders (Heath, $t_{\rm rec} = 0.07$ s) and cup-anemometers (KNMI 018). In the period from 1978 to 1983 1-min averages and gusts were collected. From these 1-min records, averages and gusts were composed for 10-, 30-, and 60-min periods. For these values of T both gustiness models were used to compute the exposure corrections. Here G will increase with increasing T. If the gustiness models express u_x as a function of T correctly, S will be the same for different values of T.

Results for one mast (# 27) are plotted in Figs. 8a and 8b. Beljaars's exposure corrections are larger for larger T. So G increases stronger with T than would be expected from Beljaars's model. The difference between $T = 600$ s and $T = 3600$ s is usually smaller than 5%. Wieringa's model gives higher exposure corrections for $T = 1800$ s than for $T = 3600$ s and $T = 600$ s. On average the difference between the curves is smaller than for Beljaars's model. The difference is a function of G, however. For large T, S is more sensitive to G than for small T. This is the result of the term $A\,(f_T - 1)$ in the denominator of Eq. (37). The larger T and f_T, the smaller the denominator becomes, and so Eq. (37) becomes more sensitive to changes in G.

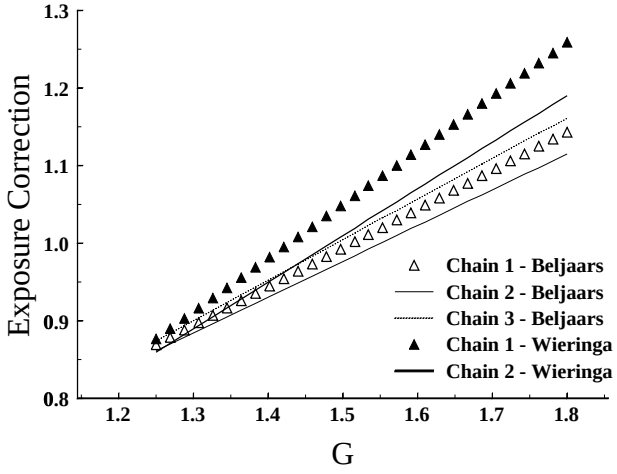

(a) $T = 3600$ s.

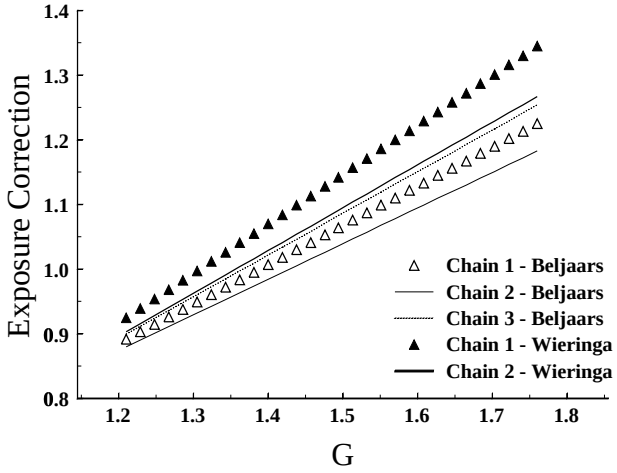

(b) $T = 600$ s.

Figure 7: Exposure correction factor S as function of G calculated using Beljaars's and Wieringa's model for the three measuring chains of section 6a with different values for $T =$ 3600 s and $T = 600$ s.

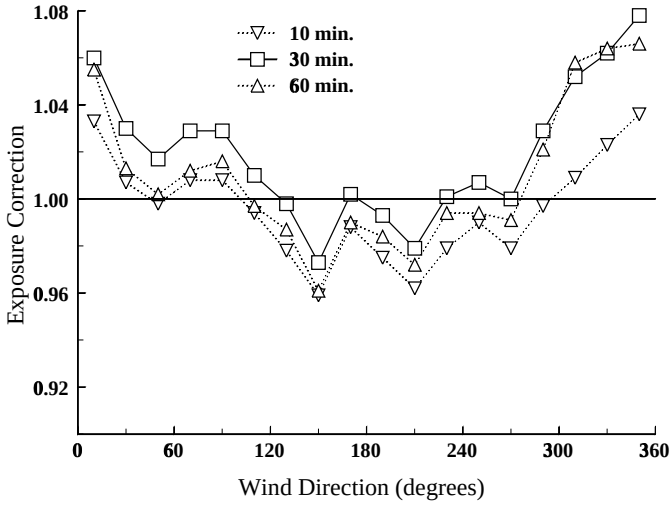

(a) Wieringa.

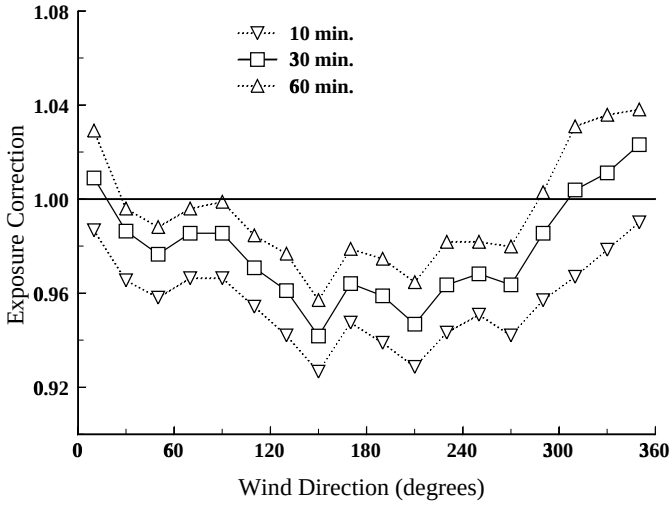

(b) Beljaars.

Figure 8: Exposure correction factor S for different values of T (600 s, 1800 s, 3600 s) calculated with Wieringa's and Beljaars's model for mast 27 of the Schiphol dataset.

c. Recorder exchange at Zestienhoven

At Zestienhoven airport during 1988 a slow recorder (Nieaf, $t_{\rm rec} = 0.8$ s) was replaced by the faster Camille Bauer ($t_{\rm rec} = 0.2$ s). This resulted in an increase in G: for wind speeds larger than 7 m s^{-1} and from the directions between 270° and 300° G increased from 1.43 ± 0.02 before 1988, to 1.55 ± 0.02 after 1988. The median was about 3% smaller than the average of G probably due to nonstationarity, which increases the average more than the median of G. Assuming that there were no significant changes in the station's surrounding, the roughness lengths found from the gustiness analysis ought to be the same before and after the recorder exchange.

The average wind speed, measured at 10-m height, in this data selection is 9.3 m s^{-1}. The response length of the cup-anemometer is 2.9 m. From this information, u_x can be computed for the measuring chains before and after the recorder exchange. The results are summarized in Table 3. It is clear that besides the small difference in roughness length between the two models, for both models a jump in z_0, and hence in S, remains. An increase of 4% in S results from straightforward application of the models. The selected sector is covered mainly by short grass close to the tower. In the distance ($\approx$ 0.8 km), however, there are some bushes and low trees. From a roughness literature review (Wieringa 1993) we expect to find a roughness length of 0.02–0.06 m. The computed roughness lengths are in the expected range.

	Before 1988		After 1988	
	Beljaars	Wieringa	Beljaars	Wieringa
$t_{\rm rec}$ (s)	0.8	0.8	0.2	0.2
A	0.90	0.88	0.93	0.92
G	1.43	1.40	1.55	1.52
u_x	3.48	2.00	3.64	2.25
z_0 (m)	0.016	0.022	0.045	0.053
S	0.98	0.99	1.02	1.03

Table 3: Measuring chain parameters and gustiness analysis of station Zestienhoven before and after the recorder exchange in 1988.

Although a 4% uncertainty in exposure correction will be acceptable for most applications, we can still wonder why the models do not neutralize the recorder exchange effect completely. The following causes are suggested. First of all, the models can be wrong. Second, the effect of the recorder exchange on S may be contaminated with changing surface roughness in the environment of Zestienhoven. Third, the measuring chain information, and therefore u_x, is incorrect.

Wieringa (1980) already validated and applied his model using different datasets success-

fully. Beljaars (1987a) also validated the sensitivity of his model to changes of measuring chains. So the first cause is not very plausible. Environmental changes cannot be ruled out completely, but it is unlikely that a sudden change in roughness has occurred in 1 yr (G increased for all wind directions). The recorder response times are only poorly documented, so these must be suspected at first. Wieringa and Van der Veer (1976) note that there is a large uncertainty in the response time of the Nieaf recorder and it may also change in time, depending on its maintenance. Applying Beljaars's model, the Nieaf recorder should have a response time about 3.6 s to level out the roughness jump. For Wieringa's model its response time should be about 1.4 s. The difference between these response times indicates that the sensitivity of the models for the measuring chain is different. More accurate information on the measuring chain is required to judge which model performs best, however. Unfortunately none of the old recorders was kept at KNMI, so checks on the response time are no longer possible. Wieringa and Van der Veer (1976) report attenuation of the gust factor during the transmission from anemometer to recorder of 18% for some stations in the Netherlands. In case that, with the replacement of the recorder at Zestienhoven, also the signal transmission was improved, this may explain the jump in measured G.

d. Estimation of wind speed at elevated levels

Gustiness analysis is applied to find a roughness length that enables us to extrapolate the wind speed from the surface to the blending height. The model's performance can directly be tested when wind speed observations at different levels are available. Therefore, we turn to the Cabauw tower.

From the Cabauw tower two wind speed records are used. The first is measured at 10-m height by a propeller vane with $\lambda = 2.2$ m (Monna and Driedonks 1979), and a recorder with $t_{\rm rec} = 1$ s, discretely sampled every 3 s. Data were stored every 30 min. A 6-yr period is analyzed. Wind speeds in the range 7–10 m s^{-1} at 10 m were selected for the gustiness analysis and for the extrapolation of the wind speed. The second record is measured at 5.4-m height, by a sonic anemometer with pathlength 0.1 m, sampled at 10 Hz. Data were stored every 10 min. Here, a 7-month period is analyzed. Wind speeds in the range 8–12 m s^{-1} at 5.4 m were selected for gustiness analysis using Beljaars's model. The resulting roughness lengths were used to extrapolate the 10-m wind from the former dataset. No analog wind speed records are available to the author at present, so the same comparison cannot be done using Wieringa's model. However, Holtslag (1984) estimated wind speed profiles of up to 200-m height at Cabauw using surface observations only. He obtained good results using roughness lengths derived with Wieringa's gust model and surface observations to estimate atmospheric stability.

In Fig. 9 the ratio of estimated to measured wind speed at different heights is plotted as function of wind direction. The gustiness analysis is applied to the wind speed records of

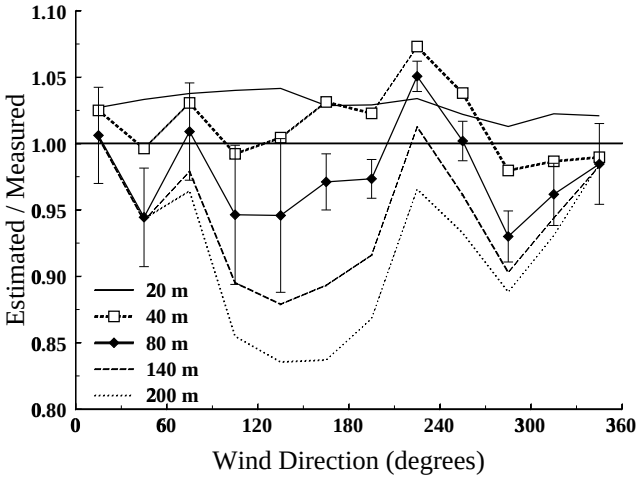

(a) z_0 from gustiness analysis of the sonic at 5.4 m.

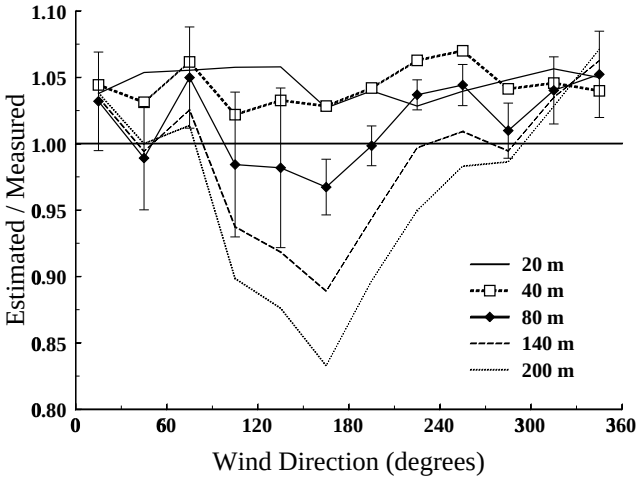

(b) z_0 from gustiness analysis of the propeller vane at 10 m.

Figure 9: Ratios of estimated to measured wind speed for different heights as function of wind direction. The wind speed profile is estimated from the wind speed measured by the propeller vane at 10-m height. The roughness length is found from gustiness analysis of a sonic at (a) 5.4-m height and (b) from the propeller vane at 10-m height (lower panel).

sonic anemometer in Fig. 9a and to the propeller vane in Fig. 9b. For the 80-m level, errors bars are plotted that denote the uncertainty in the $U_{\text{est.}}/U_{\text{meas.}}$ ratio. For clarity the error bars for the other heights are omitted but they are of the same magnitude. With the blending height assumed at a height of about 60 m, the relevant heights are the 40- and 80-m level. For both heights the estimated wind speed is within 5% of the measured wind speed, which is satisfactory. The southeast sectors, where at higher levels the largest deviations are found, is the most complex region at Cabauw.

In Fig. 9 there is a clear trend with height; the wind speed at 20 and 40 m is overestimated while at the higher levels there is a growing underestimation. Estimates based on the analysis of the 5.4-m high sensor are generally lower those that based on the 10-m high sensor. This is the result of the different footprints for the two heights (Schmid and Oke 1990). Close to the tower the surface is very smooth compared with the surface farther away. The lowest sensor will be influenced most by the surface close to the tower and the estimated roughness length will be lower. Underestimation of regional z_0 will result in underestimation of U at higher levels. Since the wind speed at 10-m height is relatively high because of the small local surface roughness, the wind speed at 20- and 40-m height will be overestimated whereas at higher levels the wind speed will be underestimated. Similar effects can also be found in the estimates of Holtslag (1984). He took into account stability effects that resulted in better wind speed estimates at higher levels. In the exposure correction procedure as applied in this paper, stability effects are not taken into account since information on stability is often not available. So there is no sense in a detailed comparison of our results with those of Holtslag (1984).

In Fig. 10 the roughness lengths are plotted as a function of wind direction. The standard Cabauw values are derived from the analysis of the standard deviation of the wind speed (Beljaars 1988), the other values are derived from gustiness analysis of the sonic anemometer at 5.4 m, and the propeller vane at 10-m height. In the east sector tree lines and a builtup area commence suddenly at about 0.3 km from the tower (see Fig. 1 of Van Ulden and Wieringa 1996). This is reflected by the high roughness lengths, although the sonic at 5.4 m seems to be influenced by the smooth local surface. The southwest sector is the most uniform and smooth sector on which all estimates agree. Going from west to north a shelterbelt-like line of low farms and trees is approaching the tower with a minimum distance of ≈ 0.5 km in the north-west direction. Farther away the surface is very smooth again. In this sector the roughness estimates do not agree at all. The sonic at 5.4 m gives the lowest roughness lengths. It is important to notice that these measurements are done 0.1–0.2 km south of the main tower. At 5.4-m height the boundary layer will be close to full equilibrium with the smooth surface in the vicinity of the tower (Garratt 1990). The approaching line of roughness elements is reflected by the increasing roughness lengths from the gustiness analysis of the propeller vane at 10-m height. In the standard Cabauw z_0 values, that is, analysis of σ_u/u_* at 10-m height, there is hardly any increase. This is probably due to different footprints for the

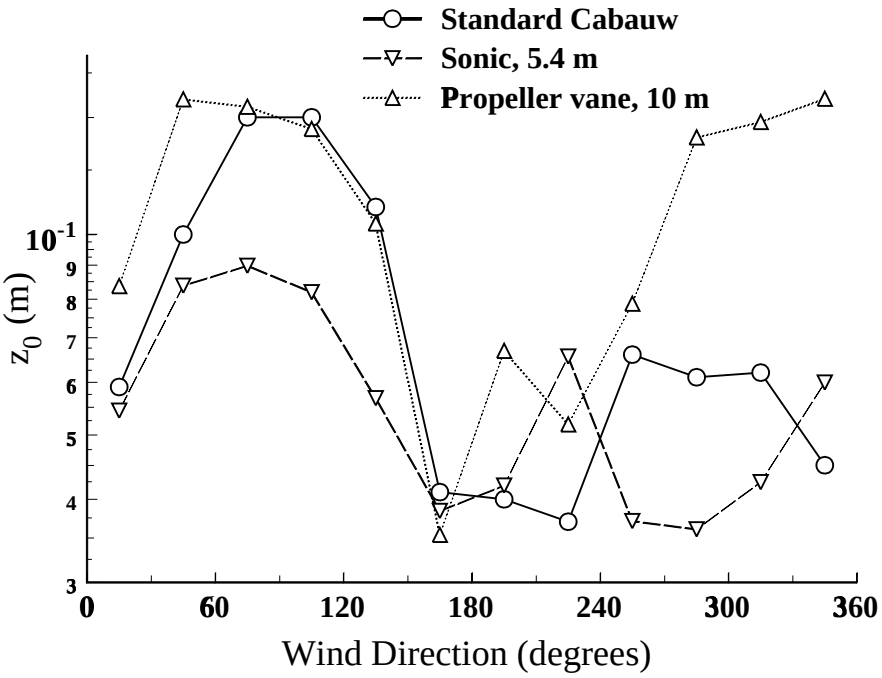

Figure 10: Roughness lengths as a function of wind direction at the Cabauw site. The standard Cabauw values are derived from the analysis of the standard deviation of the wind speed, the other values are derived from gustiness analysis of the sonic anemometer at 5.4 m, and the propeller vane at 10-m height.

extremes and the standard deviation of the wind speed signal. The standard deviation has large contributions of fluctuations with very low frequencies or large length scales. Gusts are dominated by fluctuations with higher frequency or shorter timescales. Because of the slower adaptation time of the low-frequency fluctuations, σ_u is determined by the smooth surface far upstream in the north (Højstrup 1981). So analysis of σ_u/u_* results in lower z_0 values than the gustiness analysis. Ultimately this means that the turbulent wind speed distribution cannot be Gaussian in terrain, which is strongly heterogeneous at horizontal scales of the order of 1 km.

From the estimated wind speeds in Fig. 9 in the northwest direction it can be seen that z_0 is scale dependent. For the purpose of exposure correction this implies that one should use roughness values derived from gustiness data observed at the same height as the corrected average wind, since then at least the footprint is similar. The difference between the two values observed at 10 m, the (σ_u/u_*)-derived "standard" and the propeller vane observations, requires close examination. More details of Fig. 9 can be explained by close examination of

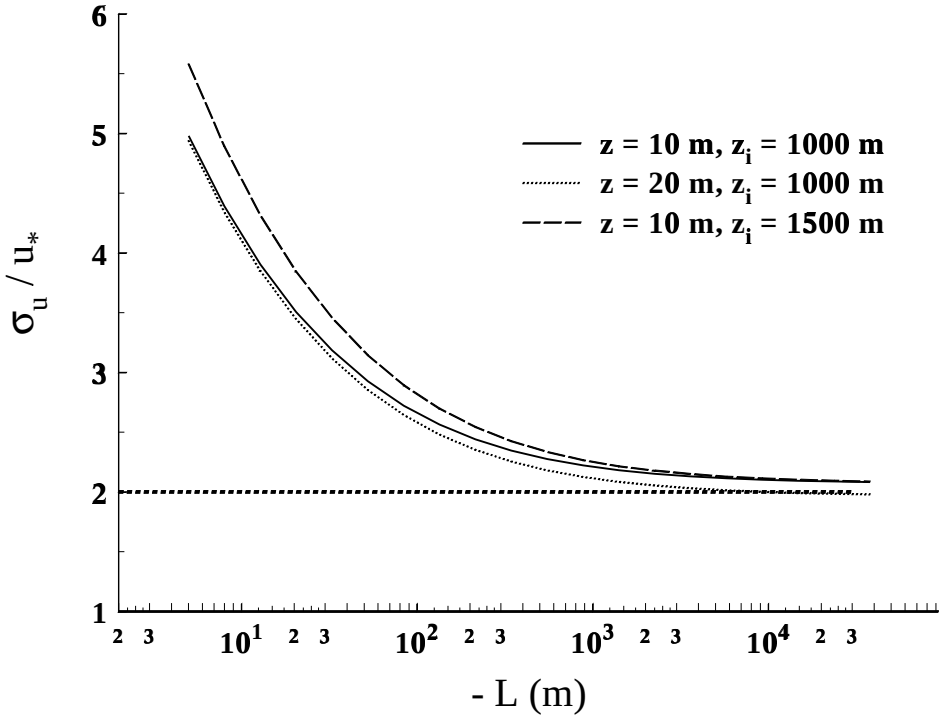

Figure 11: Standard deviation of horizontal wind speed as a function of Obukhov length for different boundary layer depths and different heights as modeled by Højstrup (1982).

the internal boundary layer structure at Cabauw, but we will not go further into this in this paper.

7. Influence of atmospheric stability and blending height

In the previous section we found a difference in exposure correction between Beljaars's and Wieringa's model of 0%–10% for gustiness analysis with $T = 3600$ s, and a difference of 2%–11% for $T = 600$ s. We found a 5% spread in S as a function of T. For the case study Zestienhoven we found a jump in exposure correction of 4% as the result of a recorder exchange, and from the Cabauw data we found that the wind speed at 40–80 m can be estimated from the gustiness and wind speed close to the surface within 5%. To put these uncertainties in exposure correction in perspective, we also consider the uncertainties resulting from atmospheric stability and the blending height estimate.

a. Influence of stability on σ_u/u_*

For the neutral surface layer, the standard deviation of horizontal wind speed fluctuations (σ_u) is related to the friction velocity (u_*). Different ratios for σ_u/u_* are reported: Beljaars used 2.2 (Panofsky et al. 1977, Beljaars and Holtslag 1991); Wieringa used 2.5, which he derived from his data over Lake Flevo ($\sigma_u/u_* = 2.47 \pm 0.52$). This corresponds also to values given by Lumley and Panofsky (1964). It is doubtful whether σ_u follows M–O theory since it is not solely determined by surface fluxes but also by eddies with the size of the atmospheric boundary layer. So σ_u/u_* will be a function of both z/L and z_i/L (Panofsky and Dutton 1984, De Bruin et al. 1993). Højstrup (1982) integrated expressions for atmospheric turbulence spectra to find a relation for σ_u/u_* as function of stability and boundary layer height (see Fig. 11):

$$\left(\frac{\sigma_u}{u_*}\right)^2 = 0.6\left(\frac{z_i}{-L}\right)^{\frac{2}{3}} + 4.8\frac{(1-z/z_i)^2}{1+15z/z_i}. \tag{38}$$

The boundary layer height z_i has only small influence on σ_u/u_*. From Fig. 11 it can be seen that σ_u/u_* at 10-m height increases from its neutral value of 2.2 to about 4 for $L = -100$ m. Stability parameters are usually not available and one often assumes a constant (neutral) value for σ_u/u_*. To determine the impact of possible errors in the estimate of σ_u/u_* on S the partial derivative of S to σ_u/u_* is taken. The sensitivity of the z_0 and S estimate for the choice of σ_u/u_* can be expressed as follows:

$$\frac{\sigma_u}{u_*} = c\left(\frac{z}{L}, \frac{z_i}{L}\right),$$

$$\frac{dz_0}{z_0} = \frac{dc}{z_0}\frac{\partial z_0}{\partial c} = -\frac{dc}{c}\left(\ln\frac{z}{z_0}\right), \tag{39}$$

$$\frac{dS}{S} = \frac{dz_0}{S}\frac{\partial S}{\partial z_0} = \frac{dz_0}{z_0}\left(\frac{\ln z_\mathrm{b}/z_\mathrm{m}}{\ln z_\mathrm{b}/z_0 \ln z_\mathrm{m}/z_0}\right). \tag{40}$$

Here dz_0 and dc represent the uncertainties in z_0 and c, respectively. With $z_\mathrm{b} = 60$ m, $z_\mathrm{m} = 10$ m, and $z_0 = 0.1$ m, the term in parenthesis in Eq. (39) equals 4.6, and that in Eq. (40) equals 0.06. With $dc = 1$ and $c = 3$, $|dz_0/z_0| \simeq 1.5$, and dS/S equals almost 0.1. For $c = 2.5$ and a dc of 0.3 ($-L > 800$ m) the uncertainty in U_p is only 2%. So the effect of nonneutral stability on the value of c is of minor importance.

b. Influence of stability on the wind speed profile

The influence of atmospheric stability on the ratio σ_u/u_* is already discussed and turned out to be of minor importance. Stability effects, however, will also influence the wind speed profile. In nonneutral, steady-state, and homogeneous conditions the wind speed gradient is a function of atmospheric stability only (Blackader and Tennekes 1968, Businger and Yaglom 1971, Obukhov 1971):

$$\frac{\kappa z}{u_*}\frac{\partial U}{\partial z} = \Phi_\mathrm{M}\left(\frac{z}{L}\right). \tag{41}$$

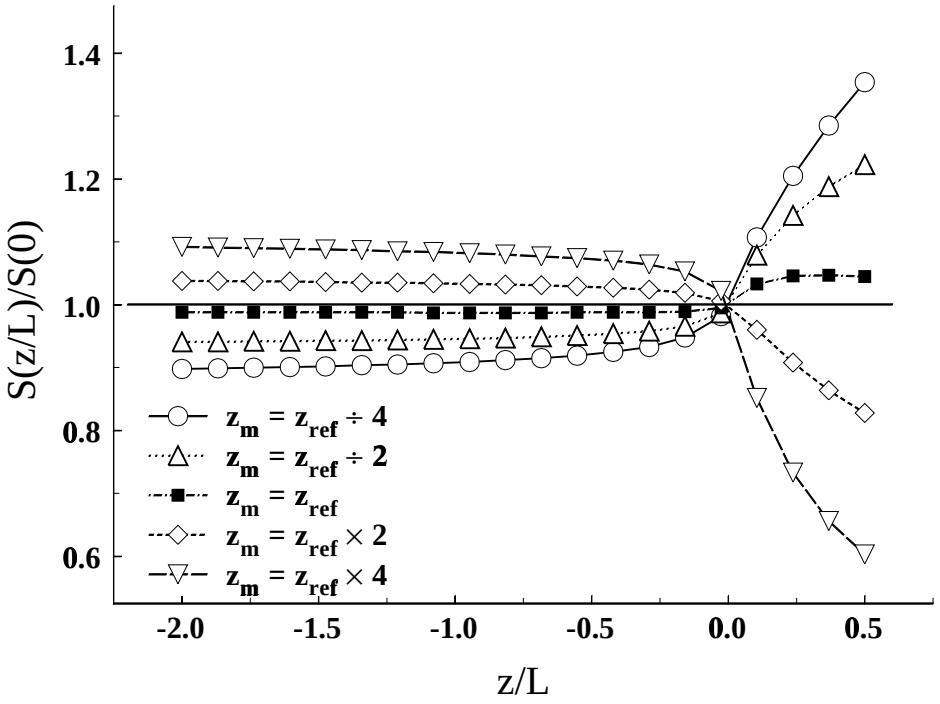

Figure 12: Effect of stability on the exposure corrections from $z_0 = 0.1$ m to $z_0 = 0.03$ m. The ratio of nonneutral to neutral exposure correction is plotted as a function of stability for different ratios of measuring height to reference height.

Here Φ_{M} is the nondimensional wind speed gradient (Dyer 1974, Yaglom 1977). Integrating this equation like in Paulson (1970) enables us to derive a nonneutral version of Eq. (5)

$$S\left(\frac{z}{L}\right) = \left[\frac{\ln z_{\mathrm{b}}/z_0 - \Psi_{\mathrm{M}}\left(z_{\mathrm{b}}/L\right) + \Psi_{\mathrm{M}}\left(z_0/L\right)}{\ln z_{\mathrm{m}}/z_0 - \Psi_{\mathrm{M}}\left(z_{\mathrm{m}}/L\right) + \Psi_{\mathrm{M}}\left(z_0/L\right)}\right] \times \left[\frac{\ln z_{\mathrm{ref}}/z_{0\mathrm{ref}} - \Psi_{\mathrm{M}}\left(z_{\mathrm{ref}}/L\right) + \Psi_{\mathrm{M}}\left(z_{0\mathrm{ref}}/L\right)}{\ln z_{\mathrm{b}}/z_{0\mathrm{ref}} - \Psi_{\mathrm{M}}\left(z_{\mathrm{b}}/L\right) + \Psi_{\mathrm{M}}\left(z_{0\mathrm{ref}}/L\right)}\right]. \quad (42)$$

In Fig. 12 the ratio of nonneutral to neutral exposure correction, $S\left(z/L\right)/S\left(0\right)$, is plotted for $z_0 = 0.1$ m. If z_{ref} is close to z_{m} the influence of stability is small. This is mainly due to the compensating effect of transforming the wind speed upward to the blending height and downward assuming the same (wrong) Obukhov length (Wieringa 1986). In unstable conditions the effect of stability on S will generally be less than 10%. In stable conditions $S\left(z/L\right)/S\left(0\right)$ soon becomes large. With $U > 5$ m s^{-1} at 10-m height, $|z/L|$ will generally be well below 0.1, and the error in S well below 10%. For larger z_0 the effect of stability is somewhat larger than for smaller roughness lengths.

c. Blending height

The blending height is a function of the horizontal scale of the major surface heterogeneity and of atmospheric stability (Mason 1988, Claussen 1990, Mahrt 1996, Philip 1997, Ma and Daggupaty 1998). For the Netherlands Wieringa (1986) used a uniform value of 60 m, corresponding to a heterogeneity length scale of a few hundred meters.

To estimate the sensitivity of S to the choice of z_b, the partial derivative of S to z_b was taken. The sensitivity of S can be expressed as follows:

$$\frac{dS}{S} = \left(\frac{\ln z_0/z_{0\mathrm{ref}}}{\ln z_\mathrm{b}/z_{0\mathrm{ref}} \ln z_\mathrm{b}/z_0} \right) \frac{dz_\mathrm{b}}{z_\mathrm{b}}. \tag{43}$$

When the local roughness is relatively small, $z_0 = 0.1$ m, $z_{0\mathrm{ref}} = 0.03$ m, and $z_\mathrm{b} = 60$ m, the expression in parenthesis equals 0.06. In this case also S itself will be close to unity, and the uncertainty in S is about 20 times smaller than that of z_b. However, if $z_0 = 1$ m, the expression in parenthesis equals 0.25. So when the local surface roughness increases, the actual value of z_b becomes more important. Using a too low z_b over rough, heterogeneous areas, which seems the most likely thing to happen, will also make S too low.

8. Conclusions

Two gustiness models, from Wieringa (1976) and Beljaars (1987a), have been evaluated and tested on their capability of relating gustiness to surface roughness. Both gustiness models assume a Gaussian distribution of the turbulent wind speed fluctuations. The computation of the exposure correction is done assuming Monin–Obukhov similarity theory is valid. Although both assumptions are common in boundary layer research, certainly in cases of heterogeneous terrain when we need exposure corrections, their validity is questionable. A theoretical objection was found against Wieringa's gust model: Wieringa applies spectral transfer functions on gusts that occur in the time domain. This results in the erroneous notion of a "gust length with maximum gust factor" for a certain measuring chain. For a certain measuring chain there will be a length- or timescale below which eddies are strongly attenuated. However, the peak gust during the observing period is always the result of the superposition of several eddies that are in phase and it cannot be associated with a single length- or timescale.

For observation periods of 1 h, Beljaars's model gives exposure corrections that are 0%–10% smaller than those from Wieringa's model, depending on surface roughness. For shorter observation periods the difference is larger. For 10-min periods, for example, Beljaars's exposure corrections are 3% to 10% smaller. In view of other uncertainties, the influence of atmospheric stability on the ratio σ_u/u_* and the wind speed profile, and the assumed blending height, the difference between the two gustiness models is small for observing periods of 1 h.

Analyzing a dataset with different values for the observing period T yields a 5% spread in exposure correction S for Beljaars's model. Here S, as calculated by the model, increases

as T increases from 600 to 3600 s. Applying Wieringa's model there seems to be a maximum in S as function of T. The spread in S is on average smaller, but the sensitivity to the gust factor G increases with T.

Both models were tested at an airport station where a change in the measuring chain has occurred, the old wind speed recorder was replaced by a faster recorder. Both models are not quite capable of leveling the change in observed gustiness. In this example a jump in roughness length remains corresponding to an exposure correction change of 4%.

Roughness lengths from Beljaars's model have been used to extrapolate the wind speed profile from 10-m height to higher levels. These estimated profiles were compared with observations from the Cabauw tower. Gustiness analysis was applied to two different wind speed records to yield the roughness length. Beljaars's model performed satisfactorily: differences less than 5% were found when estimating the wind speed at 40- and 80-m height from the wind speed at 10-m height. Since no analog wind speed records are available to the author at present, no similar analysis can be done for Wieringa's model, but Holtslag (1984) obtained good results using roughness lengths from Wieringa's gust model in combination with surface observations of atmospheric stability.

With both Wieringa's (1976) and Beljaars's (1987a) gustiness model the exposure correction can be computed with an accuracy of 5%. If this uncertainty would be due only to the uncertainty in the z_0 estimate, the uncertainty in z_0 can be found from solving Eq. (5) for z_0. It follows that the accuracy of the roughness length depends strongly on the magnitude of z_0 itself. For $z_0 = 0.03$ m it will be accurate to a factor 3–4, for $z_0 = 0.2$ m to a factor 2, and with $z_0 = 1$ m its accuracy will be about 15%.

Acknowledgments.

This paper is a partial and preliminary result of the contribution of the Royal Netherlands Meteorological Institute (KNMI) to the HYDRA project, supported by the National Institute for Coastal and Marine Management and the Institute for Inland Water Management and Waste Water Treatment.

The author wishes to thank Fred Bosveld and Rinus Rauw from the Atmospheric Research Section of KNMI, who helped computing the gust factors from the Cabauw datasets, Henk Benschop for making available the Schiphol dataset, and several members from the Observations and Modelling Section of KNMI, who also gave useful feedback. Dr. Anton Beljaars and Prof. Jon Wieringa gave helpful comments about their gust models. Prof. Wieringa also gave good advice at various stages in the writing of this paper.

References

Abramowitz, M. and Stegun, I. A., 1965: *Handbook of mathematical functions*. Dover publications, Inc.. New York.

Barthelmie, R. J., Palutikof, J. P. and Davies, T. D., 1993: Estimation of sector roughness lengths and the effect on prediction of the vertical wind speed profile. *Bound.-Layer Meteor.* **66**, 19–47.

Beljaars, A. C. M., 1987a: The influence of sampling and filtering on measured wind gusts. *J. Atmos. Oceanic Technol.* **4**, 613–626.

Beljaars, A. C. M., 1987b: On the memory of wind standard deviation for upstream roughness. *Bound.-Layer Meteor.* **38**, 95–101.

Beljaars, A. C. M., 1988: The measurement of gustiness at routine wind stations - a review. *WMO-TECO-1988*. Leipzig. pp. 311–316. WMO/TD-No. 222, also Royal Netherlands Meteorological Institute, Sc. Rep., WR 87-11.

Beljaars, A. C. M. and Holtslag, A. A. M., 1991: Flux parameterization over land surfaces for atmospheric models. *J. Appl. Meteor.* **30**, 327–341.

Blackader, A. K. and Tennekes, H., 1968: Asymptotic similarity in neutral barotropic boundary layers. *J. Atmos. Sci.* **25**, 1015–1020.

Businger, J. A. and Yaglom, A. M., 1971: Introduction to Obukhov's paper 'Turbulence in an atmosphere with a non-uniform temperature'. *Bound.-Layer Meteor.* **2**, 3–6.

Claussen, M., 1990: Area-averaging of surface fluxes in a neutrally stratified, horizontally inhomogeneous atmospheric boundary layer. *Atmos. Environ.* **24A**, 1349–1360.

De Bruin, H. A. R., Koshiek, W. and Van den Hurk, B. J. J. M., 1993: A verification of some methods to determine the fluxes of momentum, sensible heat, and water vapour using standard deviation and structure parameter of scalar meteorological quantities. *Bound.-Layer Meteor.* **63**, 231–257.

Dyer, A. J., 1974: A review of flux-profile relationships. *Bound.-Layer Meteor.* **7**, 363–372.

Frenzen, P. and Vogel, C. A., 1995: On the magnitude and apparent range of variation of the von Karman constant in the atmospheric surface layer. *Bound.-Layer Meteor.* **72**, 371–392. see also *Bound.-Layer Meteor.* **75**, 315–317.

Garratt, J. R., 1990: The internal boundary layer — a review. *Bound.-Layer Meteor.* **50**, 171–203.

Greenway, M. E., 1979: An analytical approach to wind velocity gust factors. *J. Ind. Aerodyn.* **5**, 61–91.

Højstrup, J., 1981: A simple model for the adjustment of velocity spectra in unstable conditions downstream of an abrupt change in roughness and heat flux. *Bound.-Layer Meteor.* **21**, 341–356.

Højstrup, J., 1982: Velocity spectra in the unstable planetary boundary layer. *J. Atmos. Sci.* **39**, 2239–2248.

Holtslag, A. A. M., 1984: Estimation of diabatic wind speed profiles from near-surface weather observations. *Bound.-Layer Meteor.* **29**, 225–250.

Kaimal, J. C., 1977: Horizontal velocity spectra in an unstable surface layer. *J. Atmos. Sci.* **35**, 18–24.

Kristensen, L., Casanova, M., Courtney, M. S. and Troen, I., 1991: In search of a gust definition. *Bound.-Layer Meteor.* **55**, 91–107.

Lumley, J. L. and Panofsky, H. A., 1964: *The structure of atmospheric turbulence.* Interscience. London.

Ma, J. and Daggupaty, S. M., 1998: Stability dependence of height scales and effective roughness lengths of momentum and heat transfer over roughness changes. *Bound.-Layer Meteor.* **88**, 145–160.

Mahrt, L., 1996: The bulk aerodynamic formulation over heterogeneous surfaces. *Bound.-Layer Meteor.* **78**, 87–119.

Mason, P. J., 1988: The formation of areally-averaged roughness lengths. *Quart. J. Roy. Meteor. Soc.* **114**, 399–420.

Miller, C. A., Cook, N. J. and Barnard, R. H., 1998: Calibration of the exposure of UK anemographs. *J. Wind Eng. Ind. Aerodyn.* **74-76**, 153–161.

Monna, W. A. A. and Driedonks, A. G. M., 1979: Experimental data on the dynamic properties of several propeller vanes. *J. Appl. Meteor.* **18**, 699–702.

Obukhov, A. M., 1971: Turbulence in an atmosphere with a non-uniform temperature. *Bound.-Layer Meteor.* **2**, 7–29.

Oemraw, B., 1984: Beschuttingscorrectie wind. in Dutch. *Technical Report* **TR-52**. Royal Netherlands Meteorological Institute.

Panofsky, H. A. and Dutton, J. A., 1984: *Atmospheric Turbulence, Models and Methods for Engineering Applications.* Jon Wiley & Sons. New York.

Panofsky, H. A., Tennekes, H., Lenschow, D. H. and Wyngaard, J. C., 1977: The characteristics of turbulent velocity components in the surface layer under convective conditions. *Bound.-Layer Meteor.* **11**, 355–361.

Parratt, L. G., 1961: *Probability and experimental errors in science*. Wiley. New York.

Paulson, C. A., 1970: The mathematical representation of wind speed and temperature profiles in the unstable atmospheric surface layer. *J. Appl. Meteor.* **9**, 857–861.

Philip, J. R., 1997: Blending and internal boundary-layer heights, and shear stress. *Bound.-Layer Meteor.* **84**, 85–98.

Schmid, H. P. and Oke, T. R., 1990: A model to estimate the source area contribution to turbulent exchange in the surface layer over patchy terrain. *Quart. J. Roy. Meteor. Soc.* **116**, 965–988.

Sozzi, R., Favaron, M. and Georgiadis, T., 1998: Method for estimation of surface roughness and similarity function of wind speed vertical profile. *J. Appl. Meteor.* **37**, 461–469.

Tennekes, H., 1973: The logarithmic wind profile. *J. Atmos. Sci.* **30**, 234–238.

Troen, I. and Petersen, E. L., 1989: *European Wind Atlas*. Risø National Laboratory. Roskilde, Denmark.

Van Ulden, A. P. and Wieringa, J., 1996: Atmospheric boundary layer research at Cabauw. *Bound.-Layer Meteor.* **78**, 39–69.

Wieringa, J., 1973: Gust factors over open water and built-up country. *Bound.-Layer Meteor.* **3**, 424–441.

Wieringa, J., 1976: An objective exposure correction method for average wind speeds measured at a sheltered location. *Quart. J. Roy. Meteor. Soc.* **102**, 241–253.

Wieringa, J., 1977: Wind representativity increase due to an exposure correction, obtainable from past analog station records. *WMO-Rep. No. 480 (Proc. TECIMO Conf.)*. pp. 39–44.

Wieringa, J., 1980: Representativeness of wind observations at airports. *Bull. Amer. Meteor. Soc.* **61**, 962–971.

Wieringa, J., 1986: Roughness-dependent geographical interpolation of surface wind speed averages. *Quart. J. Roy. Meteor. Soc.* **112**, 867–889.

Wieringa, J., 1993: Representative roughness parameters for homogeneous terrain. *Bound.-Layer Meteor.* **63**, 323–363.

Wieringa, J., 1996: Does representative wind information exist?. *J. Wind Eng. Ind. Aerodyn.* **65**, 1–12.

Wieringa, J. and Rijkoort, P. J., 1983: *Windklimaat van Nederland.* Staatsuitgeverij. Den Haag, the Netherlands.

Wieringa, J. and Van der Veer, P. J. M., 1976: Nederlandse windstations 1971-1974. in Dutch. *Report* **V-278**. Royal Netherlands Meteorological Institute.

Wolfson, M. M. and Fujita, T. T., 1989: Correcting wind speed measurements for site obstructions. *J. Atmos. Oceanic Technol.* **6**, 343–352.

Yaglom, A. M., 1977: Comments on wind and temperature flux-profile relationships. *Bound.-Layer Meteor.* **11**, 89–102.